UNIVERSITÀ DEGLI STUDI DI PADOVA

DIPARTIMENTO DI BIOLOGIA

Corso di Laurea magistrale in Molecular Biology

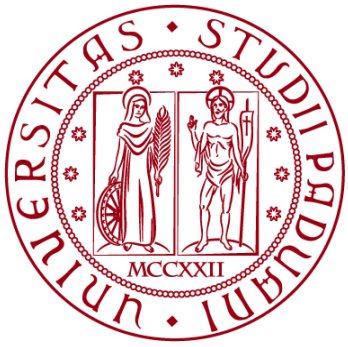

TESI DI LAUREA

C2C12: A Cell Model for Studying the Influence of Mitochondria-Induced Integrated Stress Response on Postnatal Myogenesis

Relatore: Prof. Luigi Leanza
Dipartimento di Biologia

Correlatore: Dott. Juan Diego Hernández Camacho
Struttura: Mitochondrial Biology group, Institut Pasteur, Paris, France

Laureando: Matija Kovic

ANNO ACCADEMICO 2024/2025

TABLE OF CONTENTS

ABSTRACT 2
INTRODUCTION 3
1. POSTNATAL MYOGENESIS 3
1.2. THE REGULATION OF POSTNATAL MYOGENESIS 3
1.3. POSTNATAL MYOGENESIS AND MITOCHONDRIA 5
2. MITOCHONDRIA 6
3. INTEGRATED STRESS RESPONSE 9
3.1. MITOCHONDRIA-INDUCED INTEGRATED STRESS RESPONSE 12
4. MAIN GOAL OF THE INTERNSHIP 14
MATERIALS AND METHODS 15
1. C2C12 CELL LINE 15
2. PROLIFERATION ASSAY 15
3. IMMUNOSTAINING 16
4. REVERSE TRANSCRIPTION-QUANTITATIVE PCR 16
5. KNOCKDOWN MODELS 17
6. INTEGRATED STRESS RESPONSE INDUCTION 17
7. WESTERN BLOT 18
8. IMAGE ANALYSIS 19
9. STATISTICAL ANALYSIS 20
RESULTS 21
1. FUNCTIONAL CHARACTERIZATION OF THE CELL MODEL 21
1.1. PROLIFERATION ASSESSMENT 21
1.2. DIFFERENTIATION ASSESSMENT 22
1.3. VALIDATION OF THE siRNA-MEDIATED KNOCKDOWN EFFICIENCY 23
2. PHARMACOLOGICALLY-INDUCED ACTIVATION OF THE MITOCHONDRIAL ISR 25
3. EFFECTS OF OMA1 AND LONP1 KNOCKDOWN ON THE MITOCHONDRIAL ISR ACTIVATION 27
4. EFFECTS OF THE ACTIVATED ISR ON C2C12 CELL PROLIFERATION AND DIFFERENTIATION 28
4.1 EVALUATION OF C2C12 CELL PROLIFERATION 28
4.2 EVALUATION OF C2C12 CELL DIFFERENTIATION 29
DISCUSSION 32

ABSTRACT

Postnatal myogenesis is a process of muscle tissue growth and generation that occurs after birth, typically following injury, infection, or prolonged physical activity. It begins with the activation of quiescent muscle stem cells, and ultimately leads to the formation of multinucleated myotubes and mature muscle fibers. Mitochondria play key roles during it, acting as metabolic hubs and signaling platforms. In this research, we showed the impact that mitochondrial stress-induced Integrated Stress Response (ISR) has on the postnatal myogenesis using the C2C12 mouse myoblast model. First, we performed a functional characterization of the model – confirming its capacity for proliferation, differentiation, as well as the efficient siRNA transfection. Second, we tested the pharmacological inhibitors of the electron transport chain – finding the most potent mitochondrial ISR activators in proliferation and differentiation conditions. Lastly, inducing the ISR and performing the immunostaining for specific differentiation markers, we clearly showed an impaired capacity for efficient differentiation under stress conditions. Furthermore, the knockdown of OMA1 –but not of LONP1- possessed the ability to suppress mitochondrial ISR activation. OMA1 is the very first component of the mitochondrial ISR pathway, and our preliminary results suggest that silencing it could selectively modulate ISR and block its activation.

INTRODUCTION

1. POSTNATAL MYOGENESIS

Skeletal muscle is the largest organ in the human body, representing 35 - 45 % of the total mass. It is essential for breathing, posture, locomotion, and whole-body energy homeostasis[1]. Furthermore, skeletal muscle acts as an endocrine organ that releases the specific proteins, called myokines, which once in the bloodstream, regulate normal functioning of different organs and tissues.

One of the most prominent characteristics of skeletal muscle is the capacity to adapt to physiological changes in the organism and to regenerate in response to growth, physical activity, and injury[1]. Through the process of regeneration, adult muscle stem cells prevent skeletal muscle loss through the formation of new muscle fibers. These cells are situated underneath the basement membrane of the myofibers[2]. They are known as satellite cells (SCs), and are found quiescent in the normal, uninjured adult muscle[2]. During this phase, cells can be divided into two groups, myogenic stem cells and myogenic precursor cells, based on their self-renewal ability[3]. Once they are activated, usually following the muscle injury, but also due to the inflammation or prolonged physical activity, they go through several phases of activation, proliferation, and fusion, generating completely differentiated and fully developed myofibers. Myogenic stem cells exhibit asymmetric division, during which some daughter cells return to the myogenic stem cells to serve as a stem cell reserve. On the contrary, myogenic precursor cells exhibit symmetrical division, in which every daughter cell is committed to the myoblast fate and begins to differentiate[4]. This specific and tightly controlled process, extremely important for the regulation of skeletal muscle homeostasis, is called postnatal myogenesis.

1.2. THE REGULATION OF POSTNATAL MYOGENESIS

Myogenic regulatory factors (MRFs) are regarded as master transcription factors that are upregulated during the postnatal myogenesis and ensure that once activated, satellite cells commit to the myogenic lineage (Fig. 1). These factors include Myogenic factor 5 (Myf5), Myogenic differentiation 1 (MyoD1), Myogenic regulatory factor 4 (Mrf4), and Myogenin (MyoG). They regulate myogenesis by modulating the expression of both myogenic and non-myogenic genes[3]. Pax7, on the other hand, is a transcription factor often used as a marker of quiescent muscle stem cells. It targets genes involved in the maintenance of the

postnatal SCs quiescent phenotype, regulating their proliferation and blocking the differentiation[3].

Once SCs are activated, myogenic stem cells only express Pax7, with half of the daughter cells returning to the stem cell pool. On the other hand, myogenic precursor cells, along with the expression of Pax7, start to express Myf5, the very first MRF to be expressed during myogenesis, ensuring the myogenic program[3]. Pax7 has an important role at this stage, binding to promoter and enhancer regions of the Myf5 gene, inducing its expression[5]. It also possesses RNA-binding capability, thereby directly enhancing the translation of mRNA for Ccnd1 (Cyclin D1), a key regulator of the cell cycle. In this way, Myf5 further promotes early myogenesis[6]. The next MRF expressed in the initial phase of myogenesis is MyoD, a MRF that functions redundantly in specifying muscle progenitor cells with the Myf5 factor, with MyoD often compensating for the absence of Myf5. The main function of MyoD is to withdraw cells from the cell cycle by enhancing the expression of myogenin and p21. P21 inhibits cyclin-dependent kinases, which inhibit MyoD. Therefore, MyoD expression enhances MyoD activity in satellite cells in a feedback and/or feedforward manner. Continuous expression of MyoD is required to sustain muscle-related gene expression[3]. As myoblasts exit the proliferative stage and commit to differentiation, MyoG becomes the dominant regulatory factor. It plays a crucial role in terminal differentiation by promoting myoblast fusion into multinucleated myotubes, a key step in muscle fiber formation. Myogenin also regulates the expression of structural muscle proteins, such as Myosin Heavy Chain (MyHC), which are necessary for the maturation of muscle fibers. Increased MyoD expression with myogenin expression stimulates the differentiation of these cells[4]. In the later stages of differentiation, Mrf4 takes on an important role. Its primary function is in the maturation and maintenance of muscle fibers. In adult muscle, Mrf4 helps sustain muscle mass and function, ensuring proper muscle integrity over time.

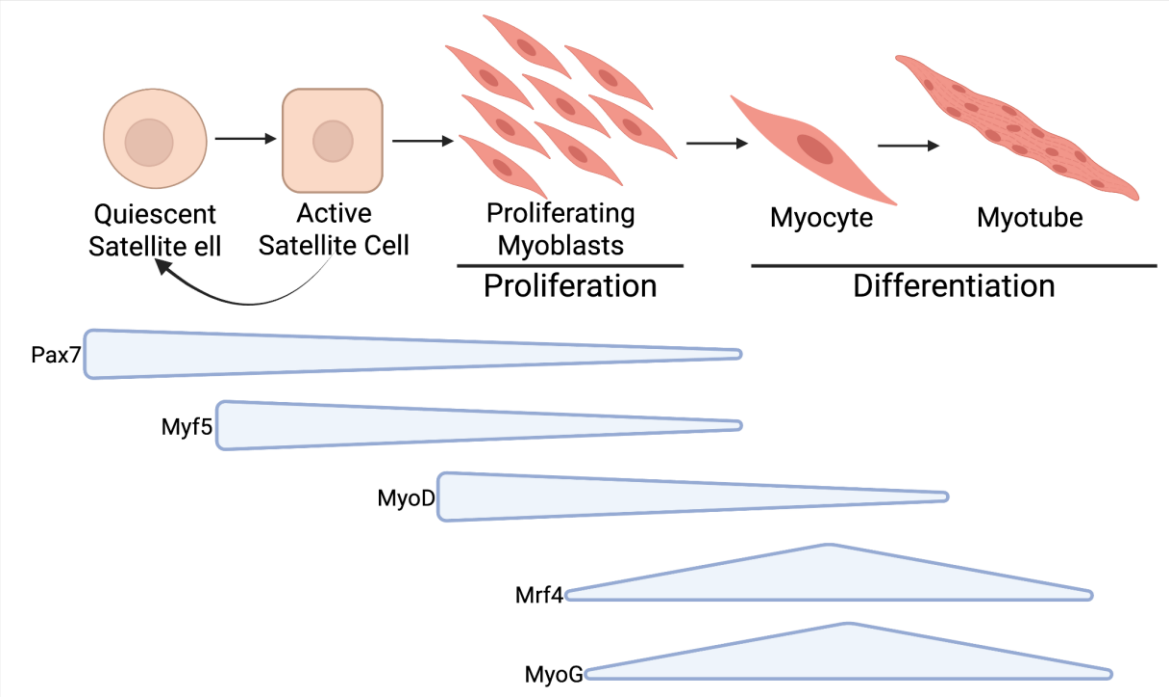

Figure 1 | Schematic Representation of Postnatal Myogenesis. Several activation signals, such as injury or inflammation, lead to SCs activation and cell cycle re-entry. Activated SCs will migrate extensively, proliferate and differentiate into myoblasts. Following several rounds of proliferation, myoblasts exit the cell cycle, becoming myocytes, which subsequently fuse to form multinucleated myotubes. This process is controlled by a genetic cascade which includes Pax7 and myogenic regulatory factors (Myf5, MyoD, Mrf4, and MyoG). Once SCs are activated, myogenic stem cells only express Pax7, with half of the daughter cells returning to the SC pool. On the other hand, myogenic precursor cells, along with the expression of Pax7, start to express MRFs. Each MRF is expressed at different time points during the process, ensuring that, once activated, satellite cells progress toward a myogenic fate.

1.3. POSTNATAL MYOGENESIS AND MITOCHONDRIA

Numerous studies support the hypothesis that mitochondrial dysfunction can have a negative impact on skeletal muscle homeostasis[7], highlighting the link between mitochondrial dysfunction and muscle loss associated with conditions such as sarcopenia and muscle atrophy, as well as prolonged physical inactivity[7,8]. Mitochondrial dysfunction can contribute to skeletal muscle wasting in at least three ways: (1) increased mitochondrial production of ROS; (2) mitochondrial release of proapoptotic factors; and (3) mitochondrial damage resulting in a reduced production of adenosine triphosphate (ATP) via oxidative phosphorylation[8]. Any disturbance in mitochondrial function can lead to an increase in reactive oxygen species levels. Elevated mitochondrial ROS production can result in permeabilization of the mitochondria outer membrane, leading to the release of pro-

apoptotic factors. One of these factors, cytochrome c, activates caspase-3 and, thus, leads to the accelerated breakdown of muscle contractile proteins and myonuclear apoptosis[8]. Furthermore, dysfunctional mitochondria exhibit an impaired capacity for oxidative phosphorylation (i.e., state 3 respiration), which can result in low ATP levels in fibers. Energy in the form of ATP is required for protein synthesis and, therefore, low energy levels in the muscle fiber could limit the production of new proteins and accelerate proteolysis. Taken together, mitochondria are crucial for maintaining cellular homeostasis and proper postnatal myogenesis. Any deviation from physiological mitochondrial function directly compromises cellular homeostasis and reduces the viability and functionality of satellite cells, myoblasts, and myocytes.

2. MITOCHONDRIA

Mitochondria are the primary oxidative units of every cell. They are intracellular double membrane-bound organelles, highly specific due to their structure and function. They generate about 90% of the total energy in the cell. This energy is produced in the form of ATP during the process of oxidative phosphorylation (OXPHOS), thanks to the respiratory chain (RC) machinery. The mitochondrial electron transport chain (ETC) supports myriad, mechanistically linked functions. It provides the driving force for ATP synthesis by oxidative phosphorylation (OXPHOS), maintains redox balance of cofactor pairs ($NADH:NAD^+$, $CoQH_2$:CoQ) that are coupled to hundreds of cellular reactions, contributes to the electrochemical gradient that drives transport of proteins and metabolites across the mitochondrial inner-membrane, and is a major determinant of cellular oxygen levels and tolerance[9]. It is important to emphasize that mitochondria are not merely the "powerhouses of the cell," as they are often referred to, but also perform numerous other roles essential for cellular physiology and function (Fig. 2a). Mitochondria are involved in the tricarboxylic acid cycle (TCA), β-oxidation of fatty acids, calcium signaling, autophagy, and many others cellular pathways. Thirteen polypeptides involved in oxidative processes, along with 22 tRNAs and two rRNAs, are encoded by mitochondrial DNA (mtDNA), which is structurally distinct from nuclear DNA (nDNA)[10]. It resembles a bacterial chromosome—it is a closed circular double-stranded DNA molecule, and as such, it can be found in almost all metazoans[11].

Since the mid-20th century, due to their complexity and potential importance in numerous cellular processes, mitochondria have been a central theme of scientific research. The pioneering work of George Palade in 1953, using electron microscopy, was the first to

demonstrate the presence of two membranes on the surface of these organelles: an inner mitochondrial membrane (IMM) and an outer mitochondrial membrane (OMM)[12]. It has been proven that the aforementioned double membrane delimits two distinct compartments: the intermembrane space (IMS), located between the two membranes, and the mitochondrial matrix, delimited by the inner membrane, in which mtDNA molecules are found. The OMM is a smooth membrane on the surface of mitochondria, permeable and serving as a platform for numerous cellular signaling pathways[13]. The development of technology has revealed an impressive function of the OMM: allowing mitochondria to form a complex reticulum that interacts with other cellular components, particularly the cytoskeleton and the endoplasmic reticulum[14]. The OMM enables direct crosstalk between mitochondria and other organelles, forming a complex network essential for the normal functioning of every cell. In contrast, the IMM can be divided into two sub-compartments: an inner boundary membrane, which parallels the outer mitochondrial membrane, and the cristae - deeply convoluted invaginations that provide surface expansion and house the machinery necessary for mitochondrial respiration[15]. The 3D images clearly show that the cristae are not baffles with wide openings into the intermembrane space but rather are pleomorphic and have an extensively tubular nature[16]. Although it has been proven that the IMM can exhibit an astounding variety of morphologies[17], it serves two fundamental functions in every cell: it acts as the scaffold for the assembly and operation of the respiratory chain complexes, and provides the permeability barrier across which the respiratory machinery generates its chemiosmotic gradient[18] (Fig 2b,c).

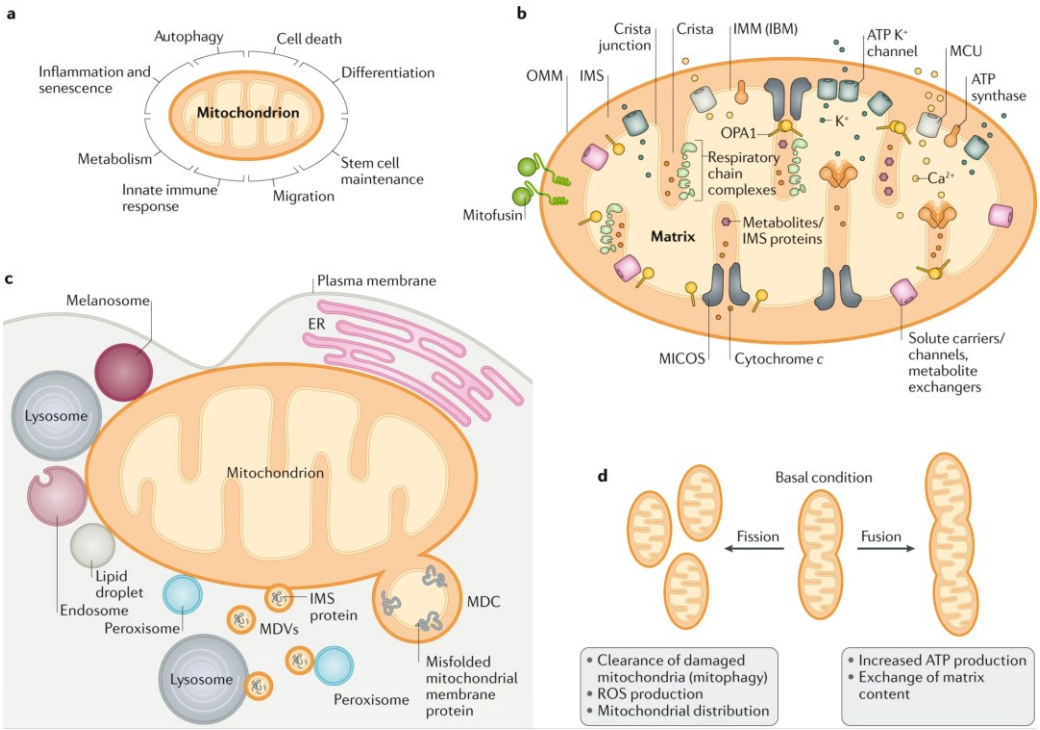

Figure 2 | Mitochondrial Structure and Function[19]**.** (a) Schematic representation of the various cellular functions of mitochondria. (b) Schematic representation of the mitochondrial structure. Mitochondrial matrix is enclosed by the outer mitochondrial membrane (OMM) and the inner mitochondrial membrane (IMM). The OMM acts as a diffusion barrier and mediates signal transduction to and from the mitochondria. The IMM consists of two main subcompartments: the inner boundary membrane (IBM) and the mitochondrial cristae. The IBM runs parallel to the OMM and houses various channel transporters. On the other hand, mitochondrial cristae are membrane invaginations that serve as sites for oxidative phosphorylation (harboring respiratory chain complexes and ATP synthase), mitochondrial DNA maintenance, and iron-sulfur cluster biogenesis. (c) OMM establishes interaction networks with other organelles, including membrane contact sites with the endoplasmic reticulum (ER), plasma membrane, lysosomes and endosomes, lipid droplets, peroxisomes, and melanosomes. These membrane contact sites regulate functions of mitochondria. (d) Schematic representation of mitochondrial fusion and fission. Fused mitochondria are able to exchange matrix contect and are capable of more efficient ATP production. On the other hand, fragmented mitochondria are harmful for cells due to the increased production of reactive oxygen species (ROS) and, therefore, are removed by mitophagy. However, mitochondrial fragmentation is required for equivalent distribution of mitochondria to daughter cells during cell division. Images taken from Giacomello et al., 2020.

Mitochondrial morphology varies widely across different cell types and tissues, throughout the cell cycle, and in response to metabolic or cellular signals[20]. They are dynamic organelles that constantly fuse and divide (Fig. 2d). These processes (collectively termed as mitochondrial dynamics) are important for mitochondrial inheritance and the maintenance of mitochondrial functions[21]. The most important mitochondrial proteases involved in the

control of mitochondrial dynamics are YME1L1 and OMA1. They regulate mitochondrial fusion and fission by a proteolytic cleavage of OPA1 protein. Its long form, known as L-OPA1, is necessary for proper fusion, while its short form, or S-OPA1, is associated with fission[22]. While YME1L1 mitochondrial protease regulates mitochondrial dynamics in physiological conditions, OMA1 is activated under stress conditions (such as oxidative and heat stress, or mitochondrial depolarization) and leads to the complete conversion of OPA1 into short forms thus promoting mitochondrial fragmentation[22]. Moreover, dysfunctional protein quality control can indirectly activate OMA1 protease. The main mitochondrial protease involved in this process is LONP1 - highly conserved Ser peptidase with an important role in degrading misfolded, oxidized, and damaged proteins in the mitochondrial matrix[22]. Its reduced activity in mice induces alterations in mitochondrial respiration and in the OXPHOS system, further activating OMA1 and promoting mitochondrial fragmentation. Mitophagy (a special type of autophagy) further removes damaged or superfluous mitochondria that have previously been segregated from the network by mitochondrial fission[22].

3. INTEGRATED STRESS RESPONSE

The Integrated Stress Response (ISR) is an elaborate signaling pathway present in eukaryotic cells, which is activated in response to a range of physiological changes and different pathological conditions. The most common stressors that activate this cellular signaling pathway include hypoxia, amino acid deprivation, glucose deprivation, and viral infection[23]. However, cell intrinsic stresses such as endoplasmic reticulum (ER) stress, caused by the accumulation of unfolded proteins in the ER, and mitochondrial dysfunction, due to the impaired ETC function or accumulation of unfolded proteins, can also activate the ISR. Furthermore, in the context of cancer biology, the ISR can be triggered by oncogene activation[23]. Depending on the intensity of the stress signal , ISR can either upregulate genes involved in promoting cellular homeostasis or, if the stress signal is too high to comprehend, apoptosis. For example, if the stress exposure is prolonged and ER protein homeostasis is not restored, the constant activation of the unfolded protein response may initiate apoptotic cell death via the up-regulation of the C/EBP homologous protein (CHOP)[24].

The common point of convergence for all stress stimuli that activate ISR is phosphorylation of the alpha subunit of eukaryotic translation initiation factor 2 (eIF2α) on serine 51[23]. The eIF2α kinases act as early responders to disturbances in cellular homeostasis. There are four members of the family: PKR-like ER kinase (PERK), double-stranded RNA-dependent

protein kinase (PKR), heme-regulated eIF2α kinase (HRI), and general control non-derepressible 2 (GCN2). Each kinase responds to distinct environmental and physiological stresses, which reflects their unique regulatory mechanisms (Fig. 3). However, in certain contexts, overlapping or combined stress signals can lead to the activation of multiple kinases.

PERK is located in the endoplasmic reticulum (ER) membrane[23]. ER stress (e.g. due to the accumulation of unfolded proteins in the ER, or perturbations in cellular energy, calcium homeostasis, or redox status) causes the activation of PERK. The classical model proposes that upon the accumulation of misfolded or unfolded proteins in the ER lumen, GRP78 (PERK's luminal domain) becomes dissociated from PERK, leading to its autophosphorylation and activation[23]. GCN2, the next eIF2α kinase, is highly conserved from yeast to humans. Mechanistic insights into GCN2 regulation, largely derived from studies in yeast, indicate that GCN2 binds to deacylated transfer RNAs (tRNAs) via a histidyl-tRNA synthetase-related domain to become active in response to amino acid deprivation[23]. Finally, the mammalian PKR is activated mainly by double-stranded RNA (dsRNA) during viral infection, while HRI is mainly expressed in erythroid cells where it is involved in erythrocyte differentiation during erythropoiesis[23]. Regulation of HRI kinase activity by heme is mediated by the two heme-binding domains that are located in the N-terminus and the kinase insertion domain. Binding of heme to the N-terminus is stable and it co-purifies with HRI, whereas heme binding to the kinase insertion domain is reversible and inhibits HRI kinase activity[23]. Heme inhibits HRI kinase activity *in vitro* and *in vivo* by promoting disulfide bond formation between HRI monomers, keeping them in an inactive dimer conformation. However, in the absence of heme, non-covalent interactions between HRI molecules occur, resulting in an active HRI dimer[23]. HRI can also be activated by other stresses including arsenite-induced oxidative stress, heat shock, osmotic stress, 26S proteasome inhibition, and nitric oxide[23]. Interestingly, activation of HRI by these diverse stresses is independent of heme and occurs with the aid of heat shock proteins HSP90 and HSP70.

As previously explained, activation of any of the aforementioned kinases leads to phosphorylation of the alpha subunit of eIF2α. Phosphorylation of eIF2α acutely inhibits global protein synthesis but promotes the translation of specific transcription factors, such as Activating Transcription Factor 4 (ATF4) and DNA Damage-Inducible Transcript 3 (DDIT3). Once synthesized, ATF4 translocates to the nucleus, where it upregulates genes involved in promoting cellular homeostasis or, alternatively, apoptosis. ATF4 functions as a

master transcription factor and, although it primarily acts as a transcriptional activator of a cohort of genes involved in cellular stress adaptation, it can also serve as a transcriptional repressor[23].

Regarding the termination of the ISR, dephosphorylation of eIF2α is central to terminating ISR signaling in order to restore protein synthesis and normal cellular function[23]. This process is mediated by a protein phosphatase 1 (PP1) complex, which consists of a catalytic subunit (PP1C) and one of the two regulatory subunits. In mammals, phosphatase activity is regulated either by PPP1R15A (also known as GADD34), which is induced as part of the ISR, or by the constitutively expressed paralog PPP1R15B (also known as CReP, constitutive repressor of eIF2α phosphorylation), which is responsible for guiding the phosphatase to eIF2α under basal conditions.

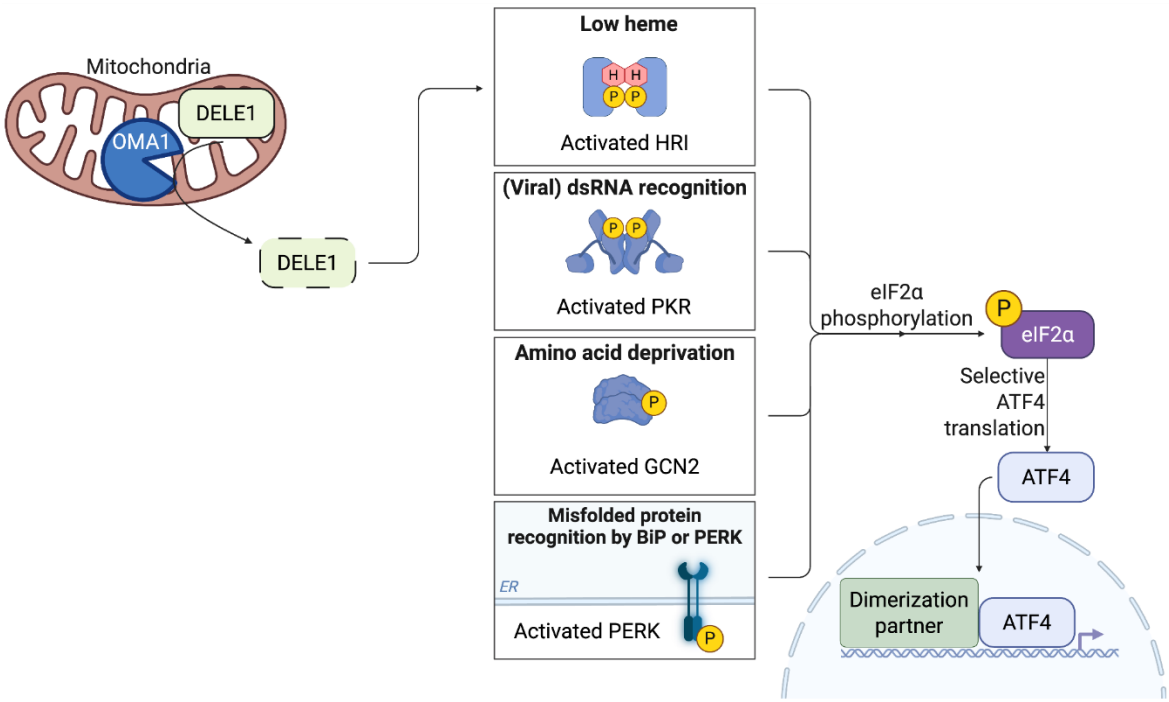

Figure 3 | Schematic representation of the Integrated Stress Response pathway. Integrated Stress Response is induced by different stress stimuli. Each stimulus is recognized by a specific protein, one of four eIF2α kinases involved in the process. However, in certain contexts, overlapping or combined stress signals can lead to the activation of multiple kinases. Once activated, these kinases ultimately lead to the phosphorylation and thus, activation of eIF2α. Furthermore, phosphorylated eIF2α increases the cellular level of ATF4, a master transcription factor of the ISR. Finally, ATF4 migrates to the nucleus where it upregulates genes involved in promoting cellular homeostasis or, alternatively, apoptosis. ER: endoplasmic reticulum.

3.1. MITOCHONDRIA-INDUCED INTEGRATED STRESS RESPONSE

In mammalian cells, the link between mitochondrial dysfunction and ISR is mediated primarily through an eIF2α kinase HRI[25]. Namely, once the proper function of mitochondria is disrupted, it stimulates the OMA1-dependent cleavage of DELE1. Therefore, OMA1 has two important functions in mitochondria: OPA1 cleavage during the mitochondrial fragmentation, and DELE1 cleavage as a response to stress conditions. DELE1 is the inner mitochondrial membrane-associated protein that, thanks to the OMA1 activity, can be found in two forms: longer form ($DELE1_L$) and cleaved form ($DELE1_S$)[25]. Whereas the longer form of DELE1 is exclusively localized in the mitochondria, $DELE1_S$ accumulates in the cytosol upon mitochondrial stress and OMA1-dependent cleavage. This cleaved form directly interacts with HRI in the cytosol and activates it. Once HRI is activated, it phosphorylates eIF2α and leads to the final activation of the ISR (Fig. 4).

OMA1 is dormant under steady-state conditions but is activated following a loss in the membrane potential[26]. On top of that, under steady-state conditions, DELE1 is imported into the matrix and continuously degraded by LONP1 - an ATP-dependent protease involved in the degradation of misfolded, damaged and oxidized proteins. LONP1 plays a key role in maintaining mitochondrial homeostasis by preventing the accumulation of toxic proteins that can induce stress. Under certain stress conditions, the decreased activity of LONP1 can accelerate OMA1-mediated DELE1 processing, leading to the ISR activation.

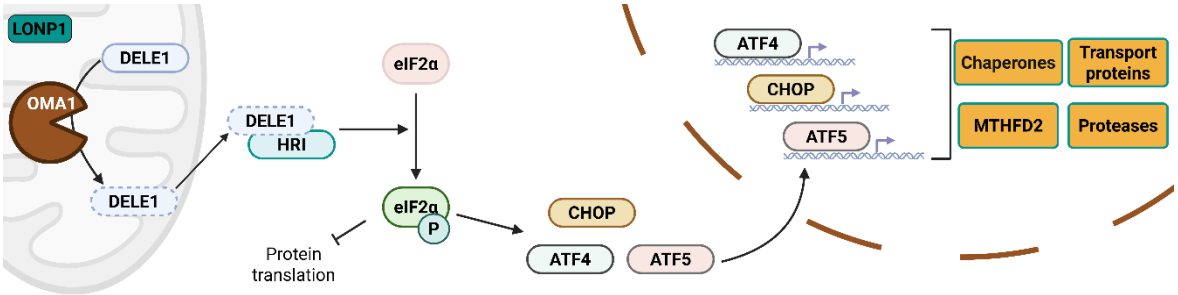

Figure 4 | Schematic representation of the OMA1-mediated Integrated Stress Response induction. Upon mitochondrial stress, activated OMA1 cleaves DELE1, whose cleaved form translocates to the cytosol. Once there, it interacts with HRI, activating it and leading to the phosphorylation of eIF2α. Phosphorylated eIF2α further increases the cellular level of ATF4, leading to the activation of the Integrated Stress Response.

Furthermore, ISR activation is usually monitored by analyzing the cellular levels of MTHFD2, a key indicator of ISR activation due to its specific role in the folate cycle. The

products of this metabolic pathway serve as precursors for nucleotide biosynthesis, required for cell proliferation and DNA replication[27]. Therefore, it is indirectly involved in the DNA damage repair, nucleotide synthesis, NADPH production, and other processes that are essential during the cellular stress response. Understandably, its promoter is a primary target of the previously activated master transcription regulator ATF4. Thus, ATF4 binding to the MTHFD2 promoter leads to the increased concentration of the MTHFD2 protein in cells under the stress condition.

Notably, knockdown of HRI—but not of DELE1 and OMA1—blocked the phosphorylation of eIF2α in cells treated with oligomycin (ATP synthase inhibitor of the electron transport chain). This finding suggests that, in addition to promoting the kinase activity of HRI under mitochondrial stress, DELE1 has a secondary role in facilitating ATF4 translation. In the absence of DELE1, mitochondrial stress still promoted the phosphorylation of eIF2α-potentially through HRI itself, by a distinct activation mechanism. Alternatively, the failure to induce ATF4 in response to mitochondrial stress in DELE1-knockdown cells might result in pervasive cellular dysfunction, leading to the activation of other eIF2α kinases[9]. What is additionally intriguing are findings from a recent study indicating that, once eIF2α is phosphorylated by HRI, it localizes on the surface of damaged and dysfunctional mitochondria, where it functions as an auxiliary “eat-me” signal in cooperation with BNIP3 and NIX receptors. In this way, phosphorylated eIF2α further promotes mitophagy and the removal of damaged mitochondria[28].

Systematic analysis revealed that there is not an universal trigger of the ISR in mitochondrial dysfunction, and rather, reveal multiple paths to its activation that depend both on the nature of the mitochondrial defect and on the metabolic state of the cell. Consequently, it was shown that besides HRI, another eIF2α kinase can link mitochondrial dysfunction to ISR activation. In proliferating myoblasts, ETC inhibition (induced by piericidin - a small Complex I inhibitory molecule) elevates the mitochondrial and cytosolic NADH/NAD+ ratios. Aspartate is largely produced from TCA cycle-derived oxaloacetate (OAA) but elevated mitochondrial NADH/NAD+ blocks the oxidative TCA cycle when complex I is inhibited. This hinders aspartate synthesis and ultimately leads to a depletion of its derivative asparagine. GCN2 is able to sense uncharged asparagine-tRNA, indicating a deficiency of free asparagine within the cell, and leading to the ISR activation. Simple asparagine supplementation is capable of blocking GCN2-mediated ISR induction[9].

4. MAIN GOAL OF THE INTERNSHIP

Using the C2C12 mouse myoblast cell line as a model system, the main goal of the internship was to understand the influence of mitochondria-induced ISR on the process of postnatal myogenesis. The understanding of the connection between these two is extremelly important for sheding light on the process of muscle regeneration, especially in the context of muscle injury, aging, and different muscle pathologies.

Postnatal myogenesis strongly depends on the proper functioning of mitochondria – it is a highly energy-dependend process that, therefore, requires their functional integrity. Recent studies have suggested that damaged mitochondria can trigger the ISR, the protective signaling pathway that modulates protein synthesis and ensures cellular homeostasis under the stress conditions. However, the consequences of ISR for skeletal muscle regeneration remain poorly understood. During this internship, we tried to understand this relationship by inducing the mitochondrial ISR and following the downstream effects it has on the C2C12 cell proliferation and differentiation. Moreover, we focused on the role of OMA1, the main mitochondrial protease involved in the induction of ISR through the proteolitic cleavage of DELE1 that consequently leads to its translocation to the cytosol and HRI activation.

The first step was to functionally characterize the cellular model. Performing the EdU assay, and MyoG/MyHC immunostaining, we managed to validate C2C12 cells proliferation and differentiation capacity. Furthermore, we developed the best protocols for C2C12 cells proliferation assessment and differentiation induction. In order to induce mitochondrial stress, we used different pharmacological inhibitors that target different complexes of the electron transport chain. Once the protocol for mitochondrial ISR was established, we performed the si-RNA mediated knockdown of OMA1 and LONP1 in order to investigate their contribution to the ISR regulation. Finally, in order to understand the impact of activated ISR on C2C12 cells proliferation and differentiation, we performed previously developed protocols for proliferation and differentiation assessments.

Overall, we managed to create a robust system for studying the interconnectivity between the mitochondrial ISR and muscle regeneration in *in vitro* conditions.

MATERIALS AND METHODS

1. C2C12 CELL LINE

C2C12 cells were obtained from ATCC (CRL-1772) and used between passages 2 and 5. Cells were cultured in high-glucose DMEM (Dulbecco's Modified Eagle's Medium, gibco) supplemented with 10 % FBS (Fetal Bovine Serum) and 1 % penicillin/streptomycin AB (antibiotics), in 5 % CO_2 at 37 °C. Cells cultured in growth medium were subcultured each time they reached 70-80 % confluency. The culture medium was replaced every two to three days. For differentiation induction, cells were cultured at higher confluency (~80 %), and the growth medium was replaced with a differentiation medium consisting of DMEM supplemented with either 2 % or 10 % HS (Horse Serum) and 1 % penicillin/streptomycin. Cells were incubated in the differentiation medium for varying lengths of time. Cells treated with therapeutic agents to induce the ISR were cultured in 10 mM low-glucose DMEM supplemented with 20 % FBS and 1 % penicillin/streptomycin, without sodium pyruvate. The differentiation medium was similar in composition, with 20 % FBS replaced by 2 % HS. Every change in cell morphology was monitored using the Nikon Eclipse Ts2 inverted light microscope.

2. PROLIFERATION ASSAY

Proliferation was evaluated by incubating the cells with the thymidine analog EdU (5-ethynyl-2'-deoxyuridine). This compound is incorporated into newly synthesized DNA and can be easily detected thanks to the small fluorescent azide present in its structure. The experiments were performed in 96-well plates, using 10,000 cells/well for each condition. After EdU incubation, cells were fixed using 4 % PFA (paraformaldehyde), washed with 3 % BSA (bovine serum albumin), and permeabilized with 0.5 % Triton X-100. For the detection of incorporated EdU, cells were treated with the Click-iT reaction cocktail (1X Click-iT® reaction buffer (0.1M Tris HCL, ph 7.0); 0.1 M $CuSO_4$; Alexa Fluor® azide; Reaction buffer additive (1 M sodium ascorbate diluted (1:20))) following the Click-iT® EdU Imaging Kits protocol (Invitrogen) in a volume of 70 µl per well for 30 minutes (protected from light). Following incubation, cells were washed with 3 % BSA, and the nuclei were stained with DAPI (Hoechst 33342, trihydrochloride, trihydrate, Invitrogen). Imaging was conducted using the Operetta microscope (PerkinElmer) with 5x and 10x magnification objectives.

3. IMMUNOSTAINING

Cells were cultured in 96-well plates, with a total number of 10,000 cells/well in proliferative condition, and 20,000 cells/well in differentiation condition. Differentiation was induced once cells became fully attached to the surface. Cells harvested at different stages of differentiation and fixed with 4 % PFA were washed in 3 % BSA and permeabilized either in 0.2 % Triton X-100 (for MyoG detection) or 0.1 % Triton X-100 (for MyHC detection). Non-specific binding was blocked by the treatment with: 10 % NGS (Normal Goat Serum) in 0.2 % Triton X-100 for 1 hour at room temperature for MyoG detection, or 10 % FBS for 1 hour at room temperature for MyHC detection. Blocking was followed by incubation with primary antibody diluted (1:30) for MyoG or (1:200) for MyHC in an appropriate blocking solution at 4 °C overnight. Cells were then incubated with the fluorochrome-conjugated secondary antibody diluted (1:500) in an appropriate blocking solution at room temperature, on the rocker, and protected from light. After brief washing in PBS (Phosphate-Buffered Saline), nuclei were stained with DAPI (Hoechst 33342, trihydrochloride, trihydrate, Invitrogen) diluted (2:5000) in PBS, for 10 minutes at room temperature, on the rocker, and protected from light.

4. REVERSE TRANSCRIPTION-QUANTITATIVE PCR

Total RNA was isolated from cells harvested at different time points of differentiation using a NucleoSpin RNA kit (Macherey-Nagel) and according to the manufacturer instructions. The RNA concentrations were determined using an Infinite® M Plex (Tecan). Subsequently, 0.45 µg of RNA/20-µl reaction mix was reverse-transcribed to cDNA using iSCRIPT cDNA Synthesis Kit (Bio-Rad). RT-qPCR was performed in a 384-well plate, with a final volume of 10 µl/well using the SYBR® Green Master Mix (Bio-Rad) on the CFX384 Touch Real-Time PCR Detection System (Bio-Rad), and with the respective primers for each gene of interest (Table 1). Cycling conditions were 1 min at 95 °C, 10 min at 95 °C, 15 s at 95 °C, and 1 min at 60 °C for 40 cycles. Gene expression was normalized to the housekeeping gene *Gapdh*, and the $2^{-\Delta\Delta CT}$ method was used for quantification.

Table 1 | List of RT-qPCR primers.

Gene	Forward primer	Reverse primer
MyoG	GAGACATCCCCCTATTTCTACCA	GCTCAGTCCGCTCATAGCC
Gapdh	AGGTCGGTGTGAACGGAT	GGGGTCGTTGATGGCAACA
β-actin	GTGACGTTGACATCCGTAAAGA	GCCGGACTCATCGTACTCC

5. KNOCKDOWN MODELS

Cells were transfected with a transfection solution consisting of: Lipofectamine RNAiMAX (Invitrogen) and siRNA [20 nM], both previously diluted in Opti-MEM™ (gibco) medium. Two siRNAs were used: one designed to complement the mRNA of interest, and the other one with a random sequence used as the negative siRNA control. Transfection solution was added on top of the seeded cells in a 6-well plate at a concentration of 100,000 cells/well and incubated in a 5 % CO_2 atmosphere at 37 °C for 48 h. The knockdown efficiency was validated by Western blotting.

6. INTEGRATED STRESS RESPONSE INDUCTION

Cells were initially treated with rotenone (a complex I inhibitor of the electron transport chain), antimycin A (a complex III inhibitor), and oligomycin (an ATP synthase inhibitor), following the proposed protocol[9]. All small-molecule inhibitors were dissolved in dimethyl sulfoxide (DMSO) (EUROMEDEX) and used at a final concentration of 1 µM. Once the cells cultured in proliferative low-glucose, no sodium pyruvate medium (explained above) were fully adhered to the surface and in a concentration of 75,000 cells/well, they were treated with pharmacological agents for either 10 hours or 24 hours. Regarding differentiating cells, once they adhered to the surface and in a concentration of 200,000 cells/well, the proliferative medium was replaced with differentiation one, inducing a differentiation process. Cells were incubated in a differentiation medium for the next 72 hours. During the final 10 hours or 24 hours of the differentiation period, cells were exposed to one of the aforementioned agents. Following treatment, cell lysates were collected, and the efficiency of ISR induction was assessed by Western blotting. Since all small-molecule inhibitors were dissolved in DMSO, it was used as a control together with the untreated (UT) cells.

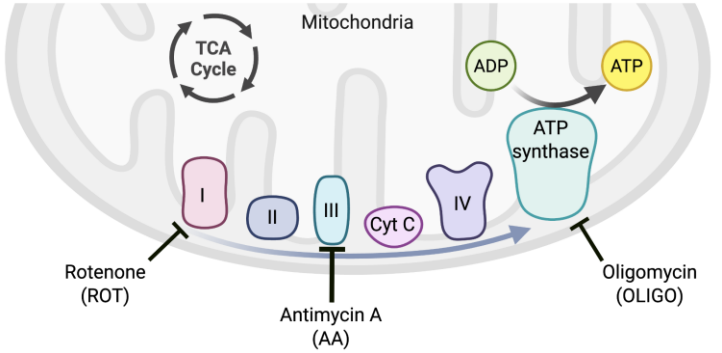

Figure 5 | Schematic representation of the effects of pharmacological agents used to induce ISR. Schematic view representing the main complexes of the electron transport chain on which drugs used have a negative effect: Rotenone (ROT) blocks the activity of complex I, Antimycin A (AA) blocks the activity of complex II, and Oligomycin (OLIGO) blocks the activity of complex IV (ATP synthase).

7. WESTERN BLOT

Cells seeded in 6-well plates were collected using 0.25 % Trypsin-EDTA (gibco) for 5 min in 5 % CO_2 at 37 °C. After trypsinization, cells were centrifuged at room temperature for 5 minutes at 2,000 rpm. The resulting pellet was homogenized in cold RIPA buffer [1 mg/20 µL; 1% Triton X-100, 1% sodium deoxycholate, 0.1% SDS, 150 mM NaCl, 50 mM Tris·HCl (pH 7.8), 1 mM EDTA, and 1 mM EGTA] and subjected to sonication using the Bioruptor® Pico (Diagenode) to enhance cell lysis and protein extraction efficiency. Sonication was performed at 4 °C for 8 cycles (30 seconds ON, 30 seconds OFF). The protein concentration was determined by Bradford assay based on Pierce™ Bradford Plus Protein Assay Reagent (Thermo Scientific), and using the Bovine Serum Albumin (BSA) standard curve. Absorbance was measured at 595 nm on Infinite® M Plex (Tecan). Equal amounts of protein from each sample were mixed with Milli-Q water and 4x Laemmli Sample Buffer [355 mM 2-mercaptoethanol, 62.5 mM Tris-HCl pH 6.8, 10% (v/v) glycerol, 1% (w/v) SDS, 0.005% (v/v) Bromophenol Blue], then heated at 95 °C for 5 minutes. Samples were loaded onto 4–20 % polyacrylamide gels (Mini-PROTEAN TGX Stain-Free gels, Bio-Rad) and subsequently transferred to a TransBlot® Turbo™ Mini-Size Nitrocellulose membrane (Bio-Rad) using the Trans-Blot® Turbo™ Transfer System (Bio-Rad). Transfer efficiency was assessed via stain-free detection. For OPA1 knockdown experiments, mPAGE Bis-Tris Gel (Millipore) was used, and Ponceau Red staining was performed to confirm efficient transfer. Gel used for OPA1 is not stain-free, and therefore a Ponecau staining is required to visualize the loading control. Membranes were blocked using 5 % (w/v) semi-skimmed dry milk dissolved in tris-buffered saline with 0.1 % Tween-20 (TBST) at room temperature for a minimum of 1 h. All primary antibodies were diluted 1:1,000 in 2 % (w/v) BSA in TBST.

Following overnight incubation in the primary antibody on a rotor and in a cold room (4 °C), membranes were washed three times for 5 min with TBST and then incubated with the secondary antibody (1:5000 in 5 % (w/v) semi-skimmed dry milk dissolved in TBST) for a minimum of 2 hours. Before protein detection using the ChemiDoc® Gel Imaging System (Bio-Rad), membranes were incubated in a chemiluminescence (ECL) solution containing 40 ml 0.1 M Tris-HCl (pH 8.5), 200 µl of 250 mM luminol, and 90 µl of 90 mM p-coumaric acid for 3 minutes on a rotor and at room temperature.

Table 2 | List of primary antibodies used.

Name	Class	Host	Manufacturer	Reference	Used for
MIC60	polyclonal	Rabbit	Proteintech	10179-1-AP	Western blot
OPA1	monoclonal	Mouse	BD Biosciences	612607	Western blot
MTHFD2	polyclonal	Rabbit	Proteintech	12270-1-AP	Western blot
LONP1	polyclonal	Rabbit	Proteintech	15440-1-AP	Western blot
MyoG	monoclonal	mouse	DSHB	AB_2146602	Immunostaining
MyHC	monoclonal	mouse	DSHB	AB_2147781	Immunostaining

Table 3 | List of secondary antibodies used.

Antigen	Host species	Dilution	Manufacturer	Reference	Target	Conjugate	Used for
Anti-Rabbit	Goat	1:5000	Fortis	A120-101P	IgG-H+L	HRP	Western blot
Anti-Mouse	Goat	1:5000	Fortis	A90-116P	IgG-H+L	HRP	Western blot
Anti-Mouse	Goat	1:500	Invitrogen	A21236	IgG-H+L	Alexa 647	Immunostaining

8. IMAGE ANALYSIS

Imaging was conducted using the Operetta microscope (PerkinElmer), and 5x or 10x magnification objectives. Software used for image analysis was Harmony High-Content Imaging and Analysis Software (revvity).

9. STATISTICAL ANALYSIS

Statistical analyses were performed in GraphPad Prism, applying either a one-way ANOVA or unpaired t-test. Data represent the results obtained from triplicate independent experiments with mean ± standard deviation (SD). ****$p<0.0001$; ***$p<0.001$; **$p<0.01$; *$p<0.5$.

RESULTS

1. FUNCTIONAL CHARACTERIZATION OF THE CELL MODEL

C2C12 is an immortalized mouse myoblast cell line that is a subclone of the mouse myoblasts originally obtained by D. Yaffe and O. Saxel. In a proliferative state, these cells have a specific radial branching morphology, with long fibers growing in different directions. Once they are cultivated in a specific medium, they exhibit high proliferative efficiency, doubling in number after approximately 24 hours of incubation. Once the differentiation is induced, they differentiate rapidly, forming contractile, multinucleated myotubes and producing characteristic muscle proteins (Fig. 6). The optimal number of days for complete differentiation is between 5 and 7 following the induction of differentiation.

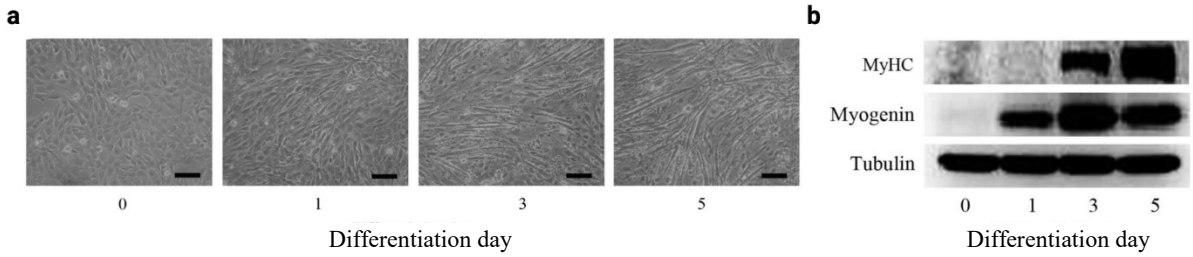

Figure 6 | C2C12 cells differentiation[29]. (a) Changes in the C2C12 morphology following the differentiation induction. At the last day of differentiation, fully differentiated myotubes are observable. (b) Changes in the expression level of characteristic muscle proteins during the differentiation process. Images taken from Zhong et al., 2016.

In the subsequent experiments, the cell model was validated and it was demonstrated that it can be successfully cultured and used for further experiments. The functional characterization included: proliferation assessment, differentiation assessment, and validation of the efficient siRNA-mediated knockdown.

1.1. PROLIFERATION ASSESSMENT

EdU was used as a measure of cell proliferation. Its detection utilizes click-chemistry – once EdU is incorporated into DNA, the Alexa Fluor azide will click to it in the presence of copper and result in a fluorescent probe.

By labelling cells with EdU at three distinct time intervals (6 hours, 4 hours, and 2 hours) in the 48 hours proliferation condition (Fig. 7a), it was possible to determine which time point is optimal for quantifying the proliferation in C2C12 cells. The potentially most effective

timepoints for accurate and reliable calculation of cell proliferation are 6 hours and 4 hours prior to cell fixation. No significant differences in total number of nuclei (Fig. 7b), and no significant differences in the number of EdU detected nuclei normalized to the total cell number (Fig. 7c), support the conclusion that, for future experiments, cells should be treated with EdU using one of these two approaches.

1.2. DIFFERENTIATION ASSESSMENT

C2C12 cells exhibit high differentiation capacity once incubated in the proper differentiation medium. During proliferation, cells were incubated in growth factor-rich conditions (high-glucose DMEM supplemented with 10% FBS). Once cells were deprived of growth factors that induce cell division, by replacing 10 % FBS with 2 % or 10 % HS, they entered the process of differentiation and fusion into multinucleated myotubes. 2 % and 10 % HS differ in the level of growth factors, which is nevertheless significantly lower than in FBS medium. Moreover, cells that remain in the proliferative medium (10% FBS) for an extended period and reach 100% confluency can exhibit signs of differentiation due to increased cell–cell interactions and lack of space for further growth.

For a more efficient and reliable representation of the investigated process - postnatal myogenesis - the most optimal differentiation protocol for inducing differentiation of C2C12 cells was determined. Cells were incubated for 48 hours under three different conditions, all assumed to promote differentiation: 2 % Horse Serum, 10 % Horse Serum, and confluent conditions (100 % confluency) in 10 % FBS. MyoG expression was analysed by immunostaining (Fig. 8a), showing the highest number of MyoG detected nuclei in the 10 % HS group (Fig. 8b). Immunostaining for MyHC (Fig. 8c) showed no significant differences in the myotube surface per well (the total area covered by multinucleated myotubes) between 2 % HS and 10 % HS protocols (Fig. 8d), indicating the same efficacy of differentiation induction. Same results were obtained for the fusion index (the number of nuclei inside the MyHC-positive myotubes divided by the total number of nuclei) (Fig. 8e), indicating the same efficacy of differentiation induction. Moreover, all protocols significantly induced differentiation compared to the proliferation control (10 % FBS, lower confluency).

In order to further validate these findings, RT-qPCR was performed. Comparison of MyoG expression levels between different groups showed no significant differences between 2 % HS and 10 % HS protocols, further indicating their equal differentiation induction abilities (Fig. 9). Finally, it was decided that the 2 % HS differentiation protocol will be used for all

subsequent experiments, but only due to its broader representation and usage in related scientific papers.

1.3. VALIDATION OF THE siRNA-MEDIATED KNOCKDOWN EFFICIENCY

Cells were incubated for 48 hours in the siRNA-transfection solution containing siRNAs specific for mitochondrial proteins MIC60 and OPA1. The level of protein expression was tested 24 hours and 96 hours upon the removal of transfection solution (Fig. 10a). Western blot analysis revealed a successful knockdown of proteins tested (Fig. 10b,c). Moreover, it was determined that protein expression gradually begins to recover 96 hours after the removal of the transfection solution, indicating that the optimal time point for using siRNA-transfected cells in following experiments is 24 hours following the transfection solution removal.

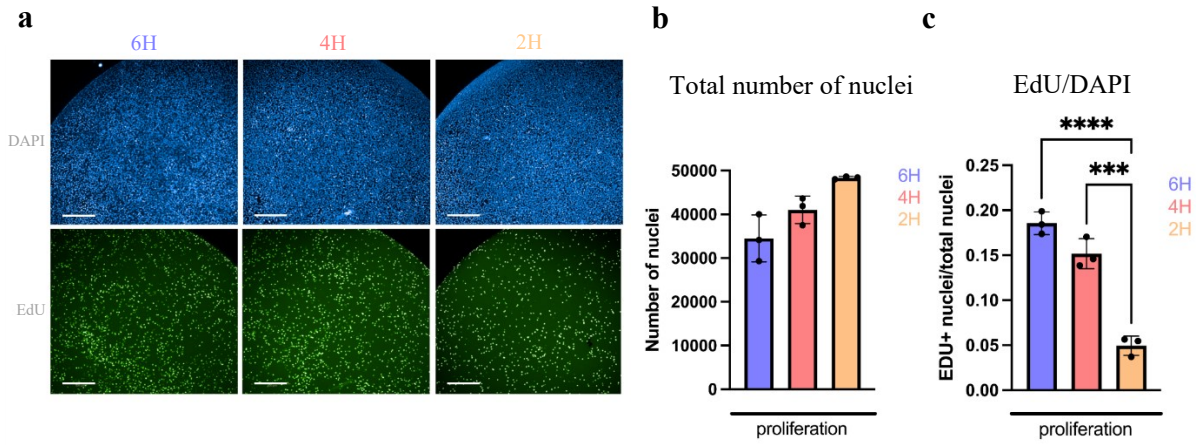

Figure 7 | Proliferation assessment. (a) Representative images of DAPI (blue) and EdU (green) staining of wild type (WT, n=3) C2C12 cells after 24 hours of proliferation. Nuclei were incubated with EdU at different timepoints (6H, 4H, and 2H) prior fixation and imaging. Scale bar, 500 μm. (b) Data represents the total number of nuclei in each group, detected by DAPI staining. (c) Ratio between the total number of EdU detected nuclei and total number of nuclei in each group. All the data (b,c) represent mean ± SD. Ordinary one-way ANOVA test was applied. n=3; ****p<0.0001; ***p<0.001.

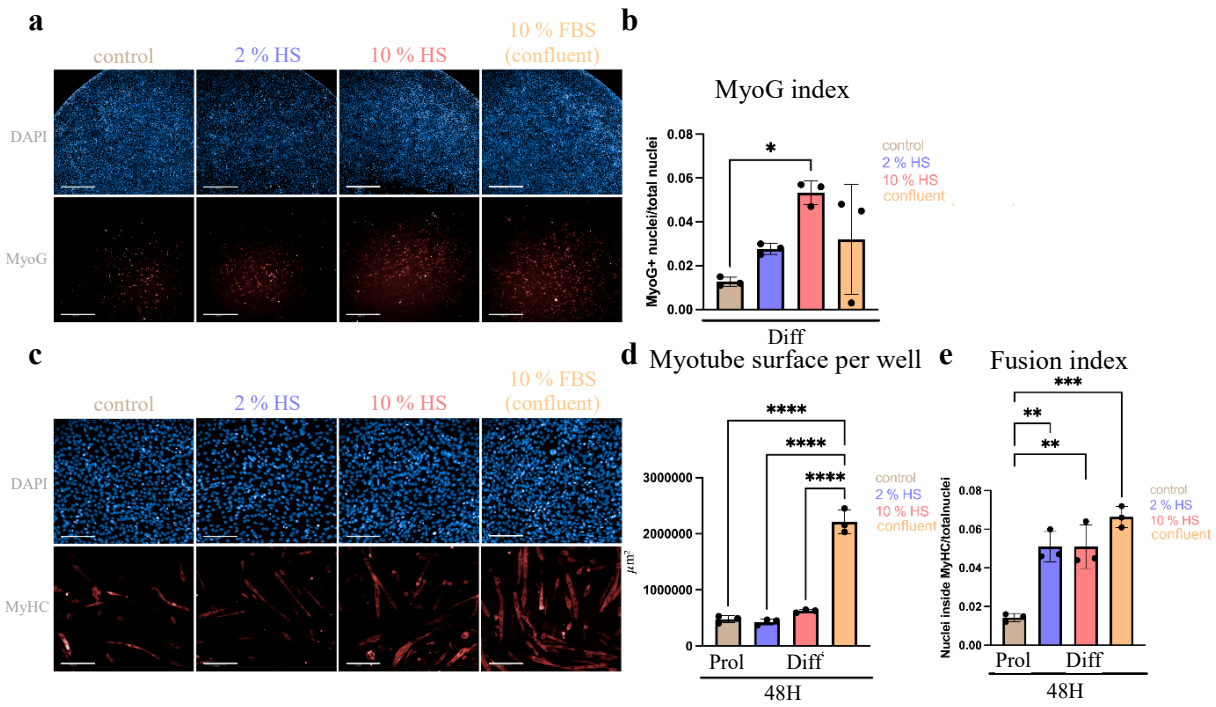

Figure 8 | Differentiation assessment. (a) Representative images of Myogenin (MyoG) (red) and DAPI (blue) IF staining of wild type (WT, n=3) C2C12 cells after 48 hours of differentiation. Scale bar, 500 µm. (b) Data represents MyoG index - the number of MyoG-detected nuclei divided by the total number of nuclei. (c) Representative images of Myosin Heavy Chain (MyHC) (red) and DAPI (blue) immunofluorescence (IF) staining of wild type (WT, n=3) C2C12 cells after 48 hours of differentiation. Scale bar, 100 µm. (d) Data represents myotube surface per well. (e) Data represents fusion index. All statistical analyses were performed in triplicates (n = 3) using the ordinary one-way ANOVA statistical test. Results are presented as mean ± SD.****p<0.0001; ***p<0.001; **p<0.01; *p<0.5. Prol: proliferation, Diff: differentiation.

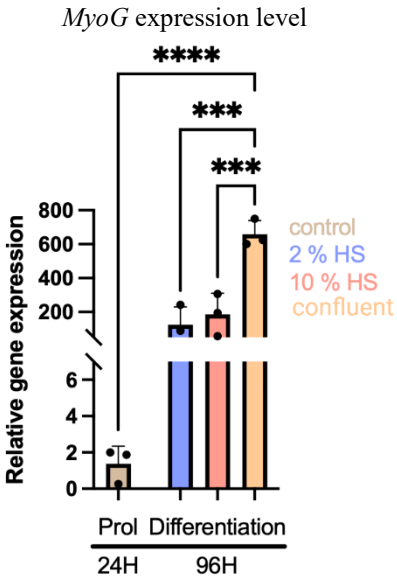

Figure 9 | Relative expression level of *MyoG*. Relative expression level was measured by RT-qPCR in wild type (WT, n=3) C2C12 cells, after 96h of differentiation. The statistical analysis was performed using the ordinary one-way ANOVA as a statistical test. Results are presented as mean ± SD.****p<0.0001; ***p<0.001.

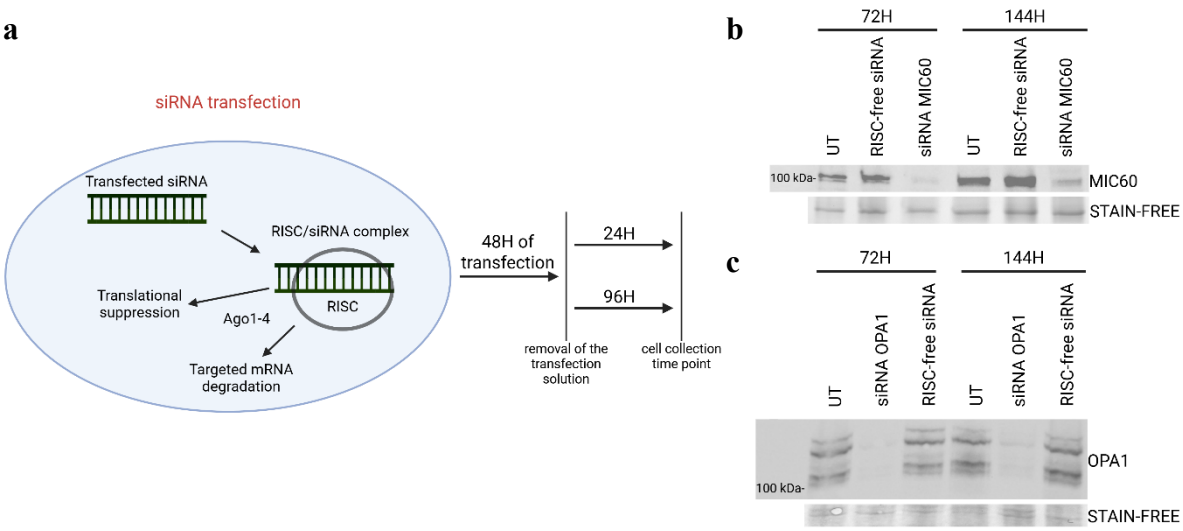

Figure 10 | siRNA-mediated knockdown validation. (a) Schematic representation of the experiment. Cells were transfected and incubated in a transfection solution for 48 hours. During this time, the formed RISC complex binds and cuts the mRNA of interest, preventing its translation into a functional protein. Then, cells were collected and prepared for the Western blot 24 hours and 96 hours after the removal of the transfection solution. (b,c) Western blots 24 hours after the removal of the transfection solution (or at a total of 72 hours after the siRNA transfection took place), and at the 96 hours time point (144 hours after the siRNA application). Both immunoblots were performed on proliferating C2C12 cells (WT, n=1). In both cases, stain-free imaging was used as a loading control for normalization.

2. PHARMACOLOGICALLY-INDUCED ACTIVATION OF THE MITOCHONDRIAL ISR

Recent studies showed that ISR can be activated using different small-molecule pharmacological inhibitors that target individual complexes of the electron transport chain[21]. In order to activate the mitochondrial ISR signaling pathway in the C2C12 cell model, three different pharmacological agents were used: rotenone, oligomycin and antimycin A. Initially, the aim was to determine which of these molecules most potently induces ISR under proliferative conditions and which one does so under differentiating conditions.

ISR activation was monitored by analyzing the cellular levels of MTHFD2, in drug-treated and untreated samples. Cells incubated under proliferative and differentiation conditions were treated with oligomycin (an ATP synthase inhibitor), rotenone (a complex I inhibitor) and antimycin A (a complex III inhibitor) at two different time points: 10 hours and 24 hours prior to cell pellet collection and preparation of material for Western blotting (Fig. 11a and Fig. 12a). It is shown that rotenone is the most effective inducer of the ISR under

proliferative conditions (Fig. 11b,c). By inhibiting complex I of the electron transport chain, rotenone increases the activity of the mitochondrial protease OMA1, enhances DELE1 protein cleavage, and activates the ISR through the HRI kinase activation. Furthermore, oligomycin seemed to be the most potent activator of the ISR in cells' ongoing differentiation process (Fig. 12b,c).

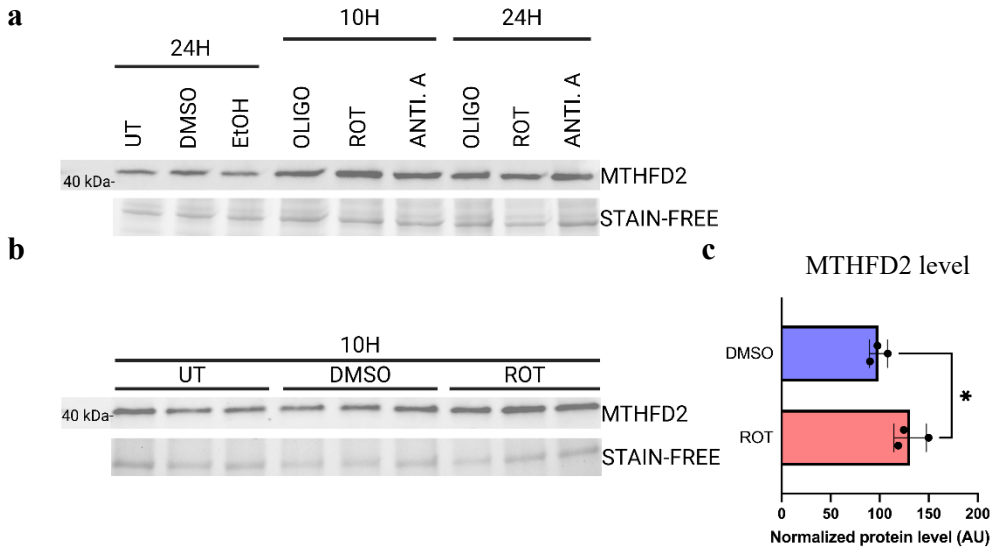

Figure 11 | ISR induction under proliferative conditions. (a) Cells were treated with 3 different drugs: oligomycin (OLIGO), rotenone (ROT), and antimycin A (ANTI.A), in proliferating conditions. The effect on ISR induction was monitored after 10 hours and 24 hours of drug exposure. n=1. (b) Immunoblot of mitochondrial protein MTHFD2 in proliferating C2C12 cells (WT, n=3) and following the 10 hours rotenone treatment. In both cases, stain-free imaging was used as a loading control for normalization. (c) Statistical analysis representing an increased MTHFD2 level following 10 hours of rotenone exposure. Data represent mean ± SD. Unpaired t test was applied. *p<0.5.

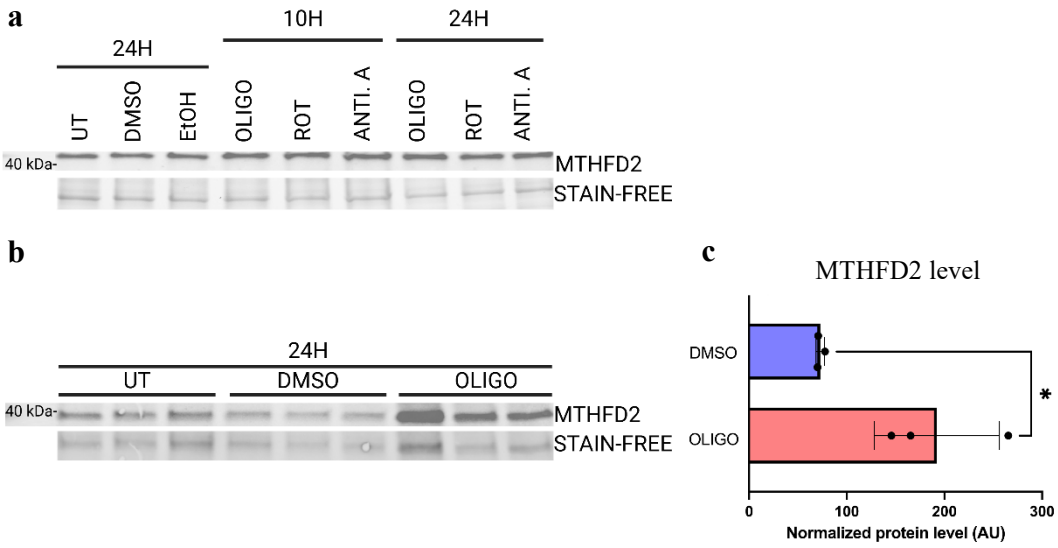

Figure 12 | ISR induction under differentiation conditions. (a) Cells were treated with 3 different drugs: oligomycin (OLIGO), rotenone (ROT), and antimycin A (ANTI.A), in differentiation

conditions. The effect on ISR induction was monitored after 10 hours and 24 hours of drug exposure. n=1. (b) Immunoblot of mitochondrial protein MTHFD2 in differentiating C2C12 cells (WT, n=3) and following the 24 hours oligomycin treatment. In both cases, stain-free imaging was used as a loading control for normalization. (c) Statistical analysis representing an increased MTHFD2 level following 24 hours of oligomycin exposure. Data represent mean ± SD. Unpaired t test was applied. *p<0.5.

3. EFFECTS OF OMA1 AND LONP1 KNOCKDOWN ON THE MITOCHONDRIAL ISR ACTIVATION

Under physiological conditions, OMA1 is dormant and not active. Following the mitochondrial stress (i.e., loss in the mitochondrial membrane potential) OMA1 becomes activated. In its active form, OMA1 cleaves mitochondrial protein DELE1, whose short form ($DELE1_s$) then translocates in the cytosol where it interacts with one of the eIF2α kinases - HRI. This interaction leads to the phosphorylation of the eIF2α and, thus, activation of the ISR signalling pathway.

It was hypothesized that OMA1 knockdown can prevent ISR activation. If OMA1 is inactivated, there is no cleavage of mitochondrial protein DELE1 and, therefore, no activation of HRI and its downstream interactors (Fig. 13a).

All cells were subjected to siRNA transfection to induce siRNA-mediated knockdown of two mitochondrial proteins — OMA1 and LONP1. Following the knockdown (KD), cells were treated with appropriate ISR activators (rotenone for proliferating cells and oligomycin for differentiating cells). It was observed that OMA1 KD prevents the increase in the concentration of the ISR activation marker protein MTHFD2, indicating its ability to block ISR induction (Fig. 13b). This finding is consistent with the proposed model and the idea that, in the absence of OMA1, DELE1 cleavage and activation of downstream factors do not occur. LONP1 KD did not show an inhibiting influence on the ISR activation.
However, OMA1 KD alone was not sufficient to prevent ISR activation under differentiation conditions. We hypothesize that oligomycin exposure may have induced cell death, and OMA1 KD was not effective enough to preserve cell viability and function (Fig. 13c).

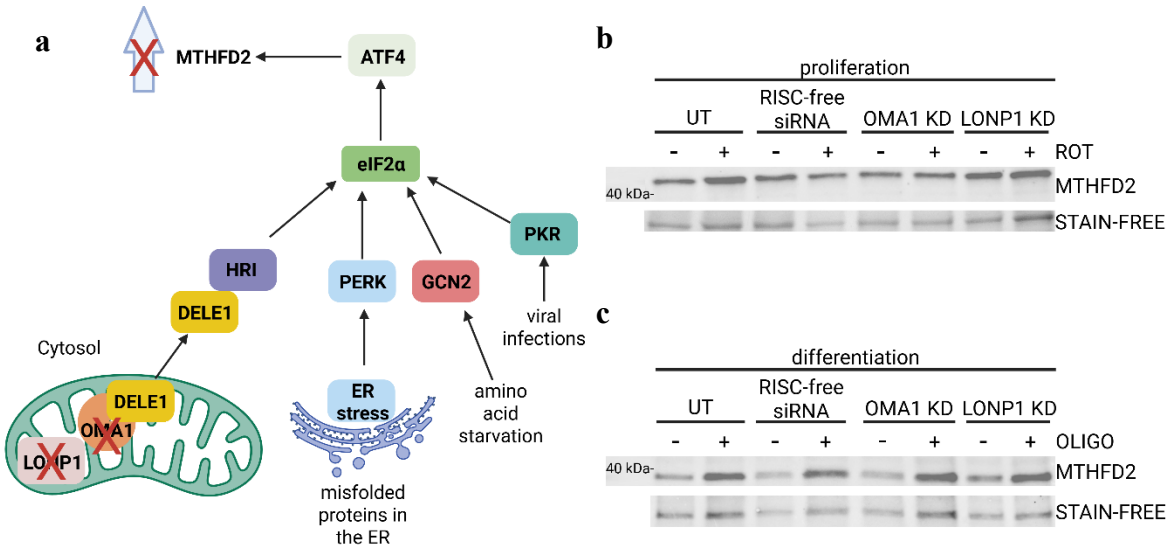

Figure 13 | Effects of OMA1 and LONP1 knockdown on ISR activation. (a) Schematic representation of the OMA1 knockdown effect on ISR activation. Once inactivated, the OMA1 protease does not cleave the DELE1 protein. Since it remains unprocessed, DELE1 does not translocate to the cytosol and, consequently, does not activate the eIF2α kinase HRI. In the absence of HRI activation, eIF2α is not phosphorylated, and thus, the integrated stress response is not induced. (b) Immunoblot of mitochondrial protein MTHFD2 in proliferating C2C12 cells with/without OMA1 or LONP1 knockdown, treated or not with rotenone (ROT). (c) Immunoblot of mitochondrial protein MTHFD2 in differentiating C2C12 cells with/without OMA1 or LONP1 knockdown, treated or not with oligomycin (OLIGO). Both immunoblots were performed on C2C12 cells (n=1) and in both cases stain-free imaging was used as a loading control for normalization. ER: endoplasmic reticulum.

4. EFFECTS OF THE ACTIVATED ISR ON C2C12 CELL PROLIFERATION AND DIFFERENTIATION

In order to understand the impact of mitochondria-induced ISR on the proliferation and differentiation of C2C12 myoblasts, and based on the observation that a 24-hour oligomycin treatment negatively affects cell viability, cells were treated only with rotenone for 10 hours in proliferation medium. Following rotenone treatment, cells were incubated for 24 hours in the proliferation medium, and for 24 hours and 48 hours in the differentiation medium (Fig. 14).

4.1 EVALUATION OF C2C12 CELL PROLIFERATION

Proliferation quantification, using the EdU reagent, did not show a significant impact on C2C12 cell proliferation following the rotenone treatment (Fig. 15a). Comparison of the total

number of nuclei (Fig. 15b), and no significant differences in the number of EdU detected nuclei normalized to the total cell number (Fig. 15c) between untreated and treated cells indicate a similar cell cycle progression efficacy.

4.2 EVALUATION OF C2C12 CELL DIFFERENTIATION

Immunostaining for MyoG and MyHC (Fig. 16a,c) revealed a strong impact of rotenone-induced ISR on C2C12 cell differentiation. Namely, cells treated with rotenone and put in the differentiation medium showed a significantly lower MyoG index (Fig. 16b) than the untreated cells, after 48 hours of differentiation. Even though there is no significant difference in myotube surface per well (Fig. 16d) between untreated and treated cells after 48 hours of differentiation, fusion index data (Fig. 16e) further support the previous conclusion, showing a lower number of nuclei present in the MyHC+ cells following rotenone treatment. These results clearly indicate incapability of C2C12 cells to properly differentiate under mitochondrial-stress conditions.

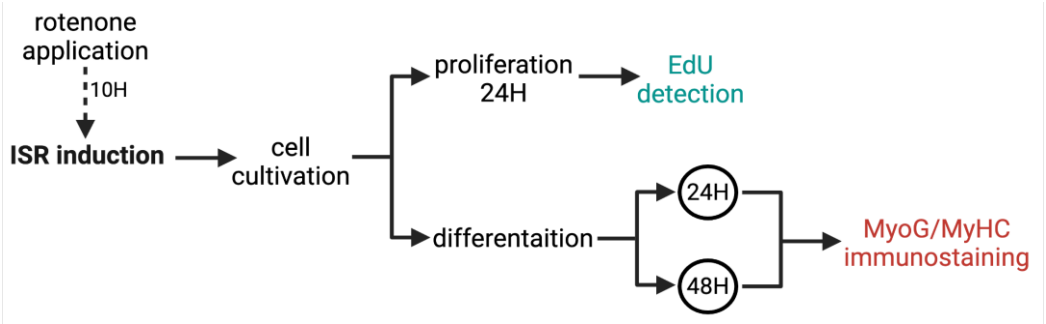

Figure 14 | Schematic representation of the final experimental setup. Cells were treated with rotenone for 10 hours and in a proliferation medium in order to induce the mitochondrial ISR. After rotenone treatment, cells were cultivated for EdU detection (24 hours in proliferation medium) and MyoG/MyHC immunostaining (24 hours and 48 hours in differentiation medium).

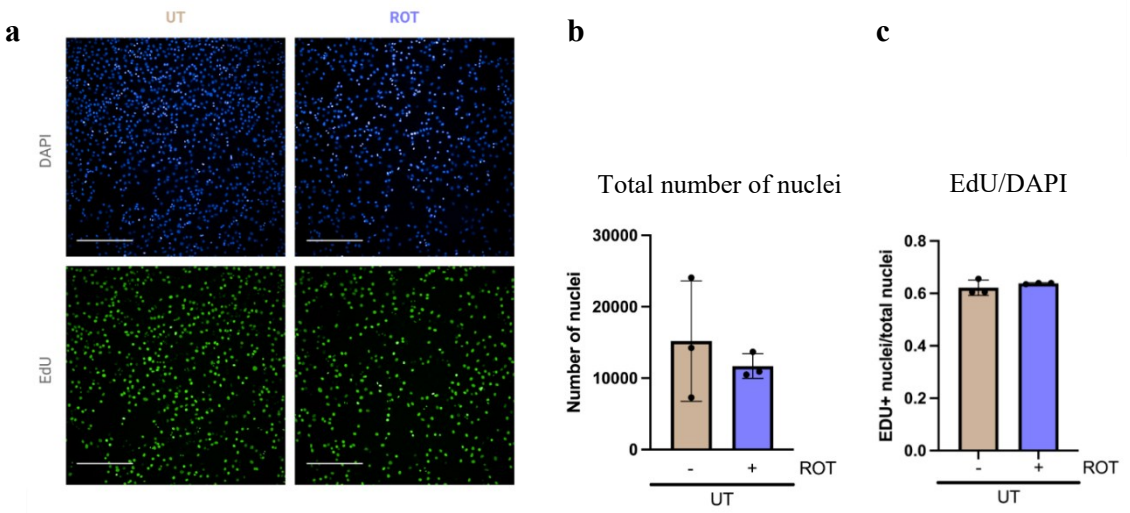

Figure 15 | Mitochondria-induced ISR doesn't have a significant impact on C2C12 cell proliferation. (a) Representative images of DAPI (blue) and EdU (green) staining of wild type (WT, n=3) C2C12 cells after 24 hours of proliferation. On the left panel are untreated, while on the right panel are rotenone-treated cells. Nuclei were incubated with EdU for 4 hours prior fixation and imaging. Scale bar, 100 µm. (b) Data represents the total number of nuclei in each group, detected by DAPI staining. (c) Ratio between the total number of EdU detected nuclei and DAPI detected nuclei. All the data (b,c) represents mean ± SD. Ordinary one-way ANOVA test was applied.

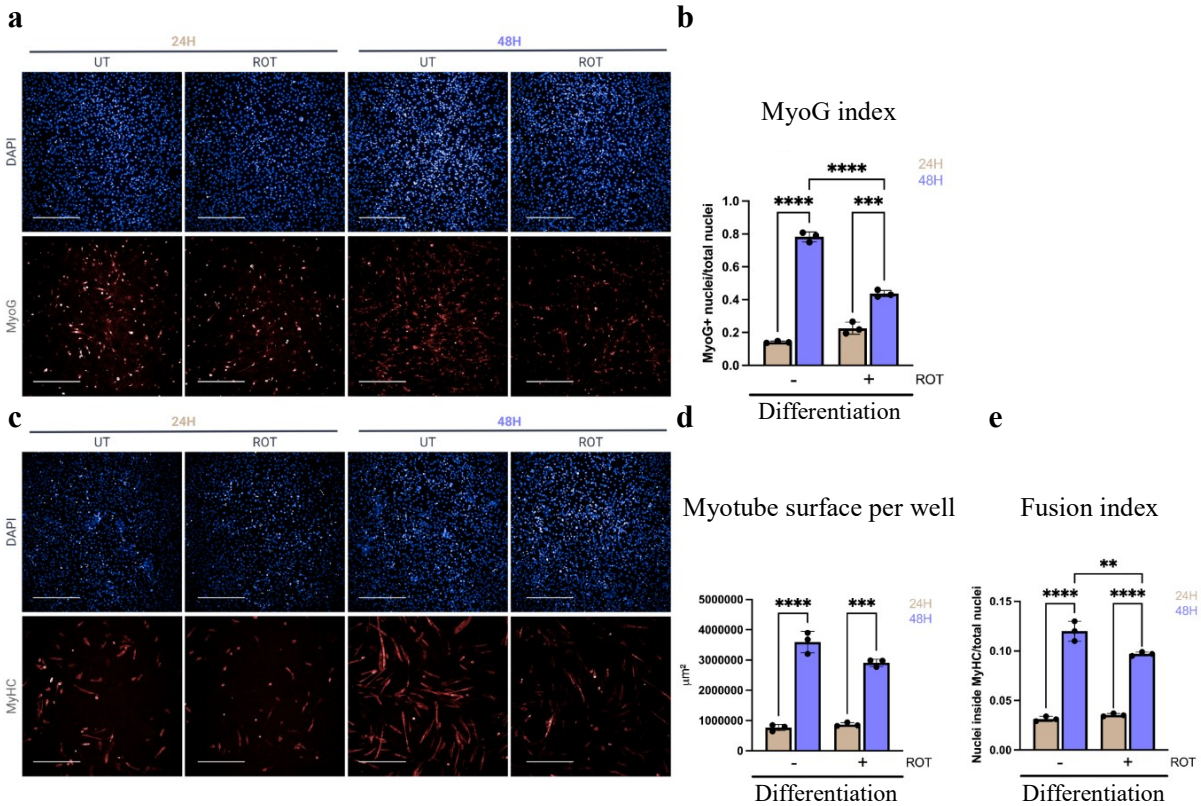

Figure 16 | Mitochondria-induced ISR has a negative impact on C2C12 cell differentiation. (a) Representative images of Myogenin (MyoG) (red) and DAPI (blue) IF staining of wild

type (WT, n=3) C2C12 cells after 24 hours and 48 hours of differentiation. First and the third column represent untreated (UT) cells, while the second and the fourth one represent cells treated with rotenone (ROT). Scale bar, 100 μm. (b) Data represents MyoG index. (c) Representative images of Myosin Heavy Chain (MyHC) (red) and DAPI (blue) IF staining of wild type (WT, n=3) C2C12 cells after 24 hours and 48 hours of differentiation. Like in the previous case, the first and the third column represent untreated cells, while the second and the fourth one represent cells treated with rotenone. Scale bar, 100 μm. (d) Data represents myotube surface per well. (e) Data represents fusion index. All statistical analyses were performed in triplicates (n = 3) using the ordinary one-way ANOVA statistical test. Results are presented as mean ± SD.****$p<0.0001$; ***$p<0.001$; **$p<0.01$.

DISCUSSION

In this work, and using C2C12 mouse myoblast as an *in vitro* model, we investigated the impact of mitochondria-induced ISR on postnatal myogenesis. Furthermore, we studied the involvement of mitochondrial protease OMA1 in regulating this signaling pathway. Understanding of the functional interplay between postnatal myogenesis and ISR is extremely important for shedding light on muscle regeneration, especially in the context of muscle injury, aging, and different muscular diseases.

ISR is not just a stress-induced signaling pathway involved in the regulation of cellular homeostasis and survival under stress conditions, but can also be the main cause of different disorders related to its imbalanced activation or deactivation. In this context, it was shown that imbalanced ISR activation can lead to severe forms of different movement disorders, such as dystonia[30]. The convergent findings of ISR dysfunction across 3 forms of dystonia was pivotal to supporting a causal role for the ISR and led to the hypothesis that weakened ISR activation is a shared pathway mechanism for dystonia . Moreover, studies on learning and memory have demonstrated that ISR manipulations restricted to neuromodulatory neurons are sufficient to alter learning and memory behavior[30]. Striatal cholinergic interneurons (CINs) represent a specific cell type characterized by increased ISR activation under basal conditions. When scientists reduced ISR activity in these neurons, they observed behavioral changes in two types of learning paradigms: instrumental task learning in lever-pressing task and spatial learning and memory recall in the Morris water maze[30]. These experiments support the idea that inhibiting or reducing CIN's ISR activity in mice leads to changes in learning and memory compared to untreated controls. Therefore, it is most likely that ISR has an important role in the regulation of these processes.

In addition to these and many other studies focusing on the activity and outcomes of prolonged, inhibited, or overstimulated ISR on physiology, there still remains a big question about how ISR influences the process of postnatal myogenesis. The incomplete understanding in this field clearly indicates the necessity for further investigation how ISR influences muscle development and regeneration.

In order to further investigate this relation, we established an *in vitro* cellular model characterized by a high capacity for both proliferation and differentiation. Very potent proliferation and rapid differentiation of C2C12 cells make it the perfect cell model for studying postnatal myogenesis. Then, using various small inhibitory molecules that target

different complexes of the mitochondrial electron transport chain, we were able to induce the ISR and investigate its downstream effects on postnatal myogenesis. Results pointed out rotenone, an inhibitor of mitochondrial complex I, as the most potent activator of the ISR under proliferative conditions. Furthermore, oligomycin, an ATP synthase inhibitor, was proved as the strongest ISR inducer in cells undergoing differentiation. Upregulation of MTHFD2, a mitochondrial enzyme involved in the folate cycle, served as the marker of successfully activated ISR.

EdU incorporation assay and MyoG/MyHC immunostainings didn't show any significant effects of mitochondria-induced ISR on C2C12 cell proliferation. On the contrary, we showed a detrimental effect of ISR activation on C2C12 cell differentiation. It was clear that C2C12 cells under stress conditions were unable to differentiate into mature myotubes. These results point out the possible incapability of tissue regeneration following the ISR activation, even though the cell cycle progression of C2C12 cells did not seem to be affected.

Is it possible to inhibit ISR activation by modulating its upstream regulators? In order to answer this question, we focused on the well-studied mitochondrial protease OMA1, known for its roles in mitochondrial dynamics regulation but not yet well-established in the context of muscle cell precursors proliferation and differentiation. Under stress conditions, OMA1 cleaves mitochondrial protein DELE1, and allows it to translocate to the cytosol and physically interact with the eIF2α kinase HRI. This interaction leads to the HRI activation, eIF2α phosphorylation and ISR activation. The role of OMA1 in regulating ISR activation is totally independent of its role in mitochondrial dynamics regulation[31]. Moreover, it was shown that its complete loss can be compensated by the increased activity of the other protein involved in the mitochondrial dynamics regulation - Parkin[31].

siRNA-mediated knockdown of OMA1 showed a significant decrease in MTHFD2 cellular levels in cells undergoing proliferation and treated with rotenone. These results pointed out the possibility of effective prevention of ISR activation by modulating the main upstream protein involved in its initiation. These results are aligned with the proposed model of OMA1-dependent DELE1 cleavage and therefore, an OMA1-dependent mitochondrial stress signaling activation. Unexpectedly, the same outcome was not observed in cells treated with oligomycin and undergoing differentiation. In this context, ISR remained active and cells experienced elevated cell death in all conditions, whether or not OMA1 was knocked down . These results support an idea that prolonged and severe stress, such as blocked ATP synthesis during differentiation, is not consistent with the ability of ISR to maintain cellular

homeostasis and protect cells from cell death. One possible explanation is that blocked ATP production leads to a drop of the cellular energetic status. Consequently, all metabolic pathways are affected, including the mitochondrial TCA cycle. Its imbalance causes a disruption in aspartate production (it is coming from the TCA cycle-derived oxaloacetate) and ultimately leads to a depletion of its derivative asparagine. Due to the ability of eIF2α kinase GCN2 to sense uncharged asparagine-tRNA (which indicates a deficiency of free asparagine within the cell), it leads to the ISR activation. Taken together, these results indicate a context-dependent role of OMA1 in ISR activation and regulation, as well as the complexity of ISR regulation and its dynamic nature.

From a translational perspective, our results emphasize a strategy to prevent and combat muscle loss in diseases linked with the mitochondrial dysfunction, such as sarcopenia, cachexia, or mitochondrial myopathies. First, we showed that OMA1 inhibition can prevent ISR activation in proliferating cells, but what is happening in differentiating ones is still not completely clear. Even though there are several papers strongly indicating OMA1's therapeutic potential - such as that OMA1 depletion in mice lacking YME1L1 (the second protease involved in OPA1 processing) can restore mitochondrial morphology and myocardial function[32], or that OMA1-DELE1-HRI axis promotes the survival of Purkinje neurons affected by spastic ataxia type 5[33]- there is a need to establish an experimental setup to follow OMA1 knockdown effects both in alive cells and *in vivo*, in the context of postnatal myogenesis. Lastly, it is important that future therapeutic efforts consider the obvious differential sensitivity of different stages of postnatal myogenesis to stress signals, side effects of potential ISR inhibition approaches, and the complexity of ISR regulation. Related to the last point, it was shown that ISR serves a protective function against ferroptosis (a specific type of cell death induced by lipid peroxidation) and delays cardiomyopathy[34]. Here, ISR promoted glutathione (GSH) synthesis and thus, an antioxidant defense through the combined activity of ATF4 and Nrf2 transcription factors. Interestingly, while ATF4 and Nrf2 activation was detected in OXPHOS-deficient heart, mild OXPHOS deficiencies in mtDNA replication-deficient skeletal muscle signal via ATF5 and manifest with a disbalance of one-carbon metabolites and nucleotides[22,34]. It thus appears that the combined and timely controlled expression of different ISR-related transcription factors in defined metabolic settings determines the stress response in a tissue-specific manner[34].

In our study we exclusively use an in vitro system, which may not accurately present the complexity of what is happening during the muscle regeneration *in vivo.* Additionally, we just focused on OMA1 and its effects on ISR regulation, leaving the open question about

possible modulations of other ISR proteins - such as DELE1, and ATF4 - in the context of postnatal myogenesis. In any case, involving genetic models and *in vivo* validation is essential to prove the relevance of these findings.

In contrast with the paper showing the positive effect of OMA1 depletion on mitochondrial morphology and myocardial function in mice lacking YME1L1, several other studies indicated negative effects of OMA1 deficiency on mitochondrial fusion–fission equilibrium and therefore, on the metabolic homeostasis. In the course of phenotypic characterization of *Oma1*-deficient mice, scientists noticed a significant increase in the body weight of *Oma1* knockout mice as compared with their wild-type littermates kept on standard chow[35]. On top of that, the cold exposure of wild-type and *Oma1* knockout brown adipose tissue (BAT) showed their impaired adaptive thermogenic response, indicating that *Oma1* ablation causes reduced energy expenditure under stress conditions[35]. Consistent with previous statements, analyzed *Oma1* knockout murine embryonic fibroblast cells (MEFs) were unable to perform the cleavage of OPA1, maintaining the mitochondrial tubular network morphology. Even though *Oma1* knockout MEFs didn't show any differences in OXPHOS function, ATP levels, or proliferation rate, they had a significant decrease in fatty-acid β-oxidation. Further analysis in brown adipocytes showed that in case of OMA1 deficiency, they were unable to perform palmitate oxidation - with OPA1 knockdown in wild-type cells showing similar results. Taken together, this indicated a pivotal role for the OMA1 protease in mitochondrial homeostasis by regulating the mitochondrial dynamics that is essential for lipid metabolism as well as to maintain body temperature and energy expenditure under cold-stress conditions[35]. Taking into account everything so far known about OMA1 function, it is clear that a deeper understanding of the tissue-specific and context-specific OMA1 function is essential - since the loss of OMA1 showed both protective outcomes in certain pathological contexts and negative metabolic disruptions in others.

To conclude:

- We established a protocol to successfully assess myogenic proliferation and differentiation of C2C12 cells in vitro.
- We optimized and validated successfull siRNA-mediated knockdown in our cellular model.
- Upon successful induction of ISR, we confirmed the negative influence of mitochondria-induced ISR on C2C12 mouse myoblasts differentiation.
- We validated the proposed model of OMA1 action during the ISR activation.
- We showed a possible way of inhibiting it by OMA1 levels manipulation.

Even though these findings have to be further validated and their relevance proved, they represent the base for future research in ISR effects on muscle regeneration and targeted interventions for muscle disorders characterized by mitochondria impairments. This work highligts the impact of mitochondrial ISR on muscle homeostasis, contributes to a better understanding of both mitochondrial ISR and postnatal myogenesis, and highlights the need for further investigation in this direction.

REFERENCES

1. Romagnoli, C., Iantomasi, T. & Brandi, M. L. Available in vitro models for human satellite cells from skeletal muscle. *Int. J. Mol. Sci.* **22**, 13221 (2021).
2. Yablonka-Reuveni, Z. Development and postnatal regulation of adult myoblasts. *Microsc. Res. Tech.* **30**, 366–380 (1995).
3. Shirakawa, T. *et al.* Factors regulating or regulated by myogenic regulatory factors in skeletal muscle stem cells. *Cells* **11**, 1493 (2022).
4. Asfour, H. A., Allouh, M. Z. & Said, R. S. Myogenic regulatory factors: The orchestrators of myogenesis after 30 years of discovery. *Exp. Biol. Med. (Maywood)* **243**, 118–128 (2018).
5. Soleimani, V. D. *et al.* Transcriptional dominance of Pax7 in adult myogenesis is due to high-affinity recognition of homeodomain motifs. *Dev. Cell* **22**, 1208–1220 (2012).
6. Panda, A. C. *et al.* Novel RNA-binding activity of MYF5 enhances Ccnd1/Cyclin D1 mRNA translation during myogenesis. *Nucleic Acids Res.* **44**, 2393–2408 (2016).
7. Nilsson, M. I. & Tarnopolsky, M. A. Mitochondria and aging-the role of exercise as a countermeasure. *Biology (Basel)* **8**, 40 (2019).
8. Hyatt, H. W. & Powers, S. K. Mitochondrial dysfunction is a common denominator linking skeletal muscle wasting due to disease, aging, and prolonged inactivity. *Antioxidants (Basel)* **10**, 588 (2021).
9. Mick, E. *et al.* Distinct mitochondrial defects trigger the integrated stress response depending on the metabolic state of the cell. *Elife* **9**, (2020).
10. Devin, A. & Rigoulet, M. Mechanisms of mitochondrial response to variations in energy demand in eukaryotic cells. *Am. J. Physiol. Cell Physiol.* **292**, C52–8 (2007).
11. Zuo, L., Zhou, T. & Chuang, C.-C. The consequences of damaged mitochondrial DNA. in *Mitochondrial Mechanisms of Degeneration and Repair in Parkinson's Disease* 49–61 (Springer International Publishing, Cham, 2016).
12. Palade, G. E. An electron microscope study of the mitochondrial structure. *J. Histochem. Cytochem.* **1**, 188–211 (1953).
13. Xian, H. & Liou, Y.-C. Functions of outer mitochondrial membrane

proteins: mediating the crosstalk between mitochondrial dynamics and mitophagy. *Cell Death Differ.* **28**, 827–842 (2021).

14. Rizzuto, R. *et al.* Close contacts with the endoplasmic reticulum as determinants of mitochondrial Ca2+ responses. *Science* **280**, 1763–1766 (1998).
15. Vogel, F., Bornhövd, C., Neupert, W. & Reichert, A. S. Dynamic subcompartmentalization of the mitochondrial inner membrane. *J. Cell Biol.* **175**, 237–247 (2006).
16. Frey, T. G. & Mannella, C. A. The internal structure of mitochondria. *Trends Biochem. Sci.* **25**, 319–324 (2000).
17. Munn, E. A. The structure of isolated mitochondria. in *The Structure of Mitochondria* 107–138 (Elsevier, 1974).
18. Mannella, C. A. Structure and dynamics of the mitochondrial inner membrane cristae. *Biochim. Biophys. Acta* **1763**, 542–548 (2006).
19. Giacomello, M., Pyakurel, A., Glytsou, C. & Scorrano, L. The cell biology of mitochondrial membrane dynamics. *Nat. Rev. Mol. Cell Biol.* **21**, 204–224 (2020).
20. Wai, T. & Langer, T. Mitochondrial dynamics and metabolic regulation. *Trends Endocrinol. Metab.* **27**, 105–117 (2016).
21. Westermann, B. Mitochondrial fusion and fission in cell life and death. *Nat. Rev. Mol. Cell Biol.* **11**, 872–884 (2010).
22. Forsström, S. *et al.* Fibroblast growth factor 21 drives dynamics of local and systemic stress responses in mitochondrial myopathy with mtDNA deletions. *Cell Metab.* **30**, 1040–1054.e7 (2019).
23. Pakos-Zebrucka, K. *et al.* The integrated stress response. *EMBO Rep.* **17**, 1374–1395 (2016).
24. Hu, H., Tian, M., Ding, C. & Yu, S. The C/EBP homologous protein (CHOP) transcription factor functions in endoplasmic reticulum stress-induced apoptosis and microbial infection. *Front. Immunol.* **9**, 3083 (2018).
25. Guo, X. *et al.* Mitochondrial stress is relayed to the cytosol by an OMA1-DELE1-HRI pathway. *Nature* **579**, 427–432 (2020).
26. Yamano, K., Kinefuchi, H. & Kojima, W. Mitochondrial quality control via organelle and protein degradation. *J. Biochem.* **175**, 487–494 (2024).
27. Ryoo, H. D. The integrated stress response in metabolic adaptation. *J. Biol. Chem.* **300**, 107151 (2024).

28. Dine, E. & Youle, R. J. Integrating the response to stressed mitochondria. *Mol. Cell* **84**, 995–997 (2024).
29. Zhong, Y. *et al.* Lrrc75b is a novel negative regulator of C2C12 myogenic differentiation. *Int. J. Mol. Med.* **38**, 1411–1418 (2016).
30. Calakos, N. & Caffall, Z. F. The integrated stress response pathway and neuromodulator signaling in the brain: lessons learned from dystonia. *J. Clin. Invest.* **134**, (2024).
31. Yamada, T. *et al.* Dual regulation of mitochondrial fusion by Parkin-PINK1 and OMA1. *Nature* **639**, 776–783 (2025).
32. Wai, T. *et al.* Imbalanced OPA1 processing and mitochondrial fragmentation cause heart failure in mice. *Science* **350**, aad0116 (2015).
33. Franchino, C. A. *et al.* Sustained OMA1-mediated integrated stress response is beneficial for spastic ataxia type 5. *Brain* **147**, 1043–1056 (2024).
34. Ahola, S. *et al.* OMA1-mediated integrated stress response protects against ferroptosis in mitochondrial cardiomyopathy. *Cell Metab.* **34**, 1875–1891.e7 (2022).
35. Quirós, P. M. *et al.* Loss of mitochondrial protease OMA1 alters processing of the GTPase OPA1 and causes obesity and defective thermogenesis in mice. *EMBO J.* **31**, 2117–2133 (2012).